Optical gain of the 1.54m emission in MBE-grown Si:Er nanolayers

Ngo, N.H.; Newell, K.; Gregorkiewicz, T.; Valenta, J.

Published in:
Physical Review B

DOI:
10.1103/PhysRevB.81.195206

Optical gain of the 1.54 μm emission in MBE-grown Si:Er nanolayers

N. N. Ha,* K. Dohnalová,† and T. Gregorkiewicz
Van der Waals-Zeeman Institute, University of Amsterdam, 65 Valckenierstraat, NL-1018 XE Amsterdam, The Netherlands

J. Valenta
Department of Chemical Physics and Optics, Faculty of Mathematics and Physics, Charles University, Ke Karlovu 3, CZ-12116 Prague 2, Czech Republic

(Received 17 September 2009; published 13 May 2010; corrected 1 June 2010)

We present investigations of the optical gain cross section of 1.54 μm Er-related emission at 4.2 K in Si/Si:Er molecular-beam-epitaxy-grown multinanolayers. This ultranarrow (full width at half maximum below 8 μeV) emission originating from the unique Er-related optical complex, Er-1 center, ensures the best condition to achieve stimulated emission. The experiments were carried out using a combination of the variable stripe length and shifting excitation spot techniques under pulsed and continuous-wave excitations. The comparison of results for both excitation regimes enables to estimate an optical gain within the strong optical losses due to the free carrier absorption. Based on these measurements, the upper limit of the optical gain cross section of 10^{-17} cm^2 and the gain coefficient of 8.8 cm^{-1} are deduced.

DOI: 10.1103/PhysRevB.81.195206 PACS number(s): 42.65.Yj, 42.65.Wi, 42.70.Hj, 42.70.Mp

I. INTRODUCTION

Realization of Si-based optical amplifiers and lasers continues to be the major challenge of Si photonics. Recent advances in this field include Si Raman laser,[1] visible laser based on Eu-doped GaN thin films on silicon,[2] and microring cavity laser.[3] These approaches, however, require external optical pumping for their operation or employ complicated manufacturing procedures. Rare-earth ion doping of Si, on the other hand, would be preferable due to relatively simple implementation into the existing Si technology and the attractive emission wavelength. Particularly interesting is Er-doped crystalline Si (c-Si:Er),[4] where the radiative transition from the first excited state ($^4I_{13/2}$) to the ground state ($^4I_{15/2}$) of Er^{3+} ions is coincident with the absorption minimum of silica fibers (c-band; 1520–1570 nm), currently used in telecommunication networks. In spite of large research efforts,[5–8] efficient amplifiers and lasers based on c-Si:Er have not yet been reported. The major problems are related to (i) the low solubility of Er in c-Si, (ii) thermal quenching, and (iii) inhomogeneous broadening of emission spectra due to multiplicity of Er-related optical centers formed in the Si host. The latter creates a situation when a photon emitted from a certain Er-related optical center is not in resonance with transitions of another center with somewhat different energy-level structure. This, together with a small absorption cross section of Er^{3+}, creates a big hurdle, and even a doubt[9] on the possibility of realization of optical amplification in c-Si:Er.

In this situation, the unique Er-related optical complex in Si/Si:Er multinanolayer structures[10] brings a promise of optical amplification. The characteristic Er-related photoluminescence (PL) spectrum from these structures at 4.2 K features only few intense and ultranarrow lines (Fig. 1). On the basis of detailed analysis of this spectrum, formation of a single type of optically active center (labeled Er-1) has been conclusively established.[11,12] When compared with broad spectra (~30 meV), typical for Er^{3+} ions in c-Si and large band-gap materials [e.g., semi-insulating polycrystalline silicon,[13] SiO_2,[14] ZnO_2, and GaN (Ref. 15)], this ultranarrow Er-1 atomiclike PL spectrum could offer a significant increase for gain coefficient, of up to 3 orders of magnitude (≈30 meV/8 μeV). Therefore, investigation of optical gain in the Si/Si:Er multinanolayer structures is particularly interesting as these materials constitute presently the most advanced form of Er-doped Si.

In this paper, we report on our study of the stimulated emission and the free carrier absorption for the aforementioned Er-1 center-related ultranarrow spectral line at 1.54 μm, using a combination of the variable stripe length (VSL) (Ref. 16) and shifting excitation spot (SES) techniques[17,18] under pulsed and continuous-wave (cw) excitations. From the observed results we derive the upper limits for the optical gain cross section and gain coefficient.

II. EXPERIMENTAL DETAILS

A. Preparation of samples

The studied Si/Si:Er multinanolayer structures were grown by a sublimation molecular-beam-epitaxy (MBE)

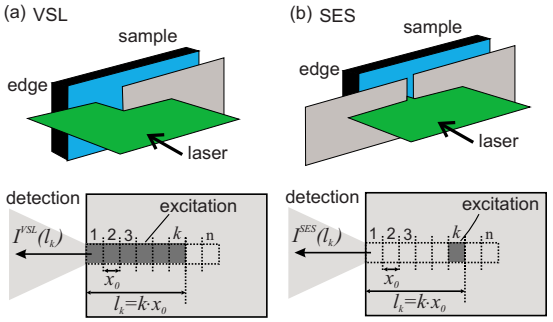

FIG. 1. (Color online) (a) The principle of the VSL and (b) SES techniques. The spot width in the SES is equal to the VSL differential shift step x_0. The emission signal is detected along the laser-exposed stripe area of length $l_k=kx_0$ ($k=0,\ldots,n$), perpendicularly to the excitation beam.

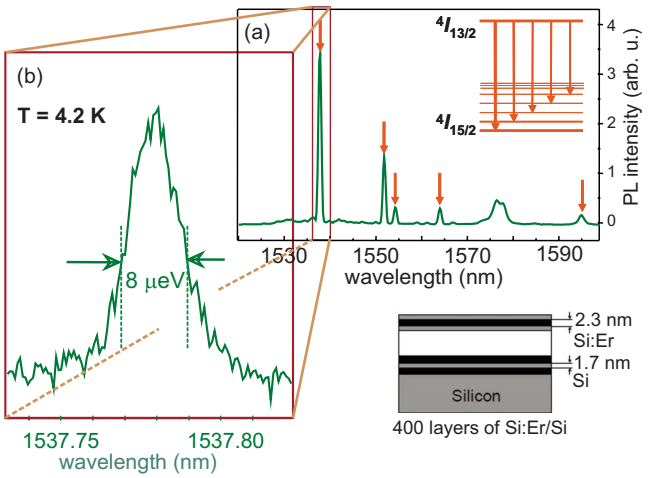

FIG. 2. (Color online) (a) PL spectrum of the Si/Si:Er multinanolayer structure, as measured at $T=4.2$ K under cw excitation at 532 nm. (b) Detail of the studied Er-1 center related ultranarrow emission line at 1.54 μm. Inset: sketch of the multinanolayer structure.

method on c-Si substrate in Institute for Physics of Microstructures, Russian Academy of Sciences (Nizhny Novgorod, Russia).[19] They comprised 400 periods of 2.3-nm-thick layers of Si doped with Er, separated by 1.7-nm-thick undoped Si layers (inset in Fig. 2). Total thickness of the epitaxial structure was around ~ 1.6 μm. The average concentration of Er^{+3} ions in the epitaxial layer was determined by the secondary ion mass spectroscopy as $[Er] \approx 3.5 \times 10^{18}$ cm^{-3}. For the optical activation of Er^{3+} ions,[19,20] the as-grown samples were annealed at 800 °C for 30 min in a continuous flow of nitrogen (5×10^{-5} cubic feet per minute, 99.99% purity). We estimate that about $\sim 25\%$ (upper limit) of all Er dopants[20] are optically active forming the Er-1 centers.

B. Low-temperature photoluminescence measurements

PL signals were studied under cw excitation at 532 nm provided by a solid-state laser $Nd:YVO_4$ (Spectra Physics). PL was detected using system of 1 m F/8 monochromator (Jobin-Yvon THR-1000; 900 grooves/mm; grating blazed at 1.5 μm) coupled with an infrared Ge detector (Edinburgh Instruments). The samples were placed in a continuous-flow He cryostat (Oxford Instruments Optistat CF) accessing the 1.5–300 K temperature range. Electronic signals from the detector were filtered and amplified via digital signal processing lock-in amplifier (Signal Recovery SR7265), and displayed by 500 MHz oscilloscope (Tektronix TDS3000).

C. Nonlinear absorption coefficient measurements—VSL and SES techniques

Stimulated emission manifests itself by a positive value of the optical gain coefficient g, which can be measured using the VSL technique originally introduced by Shaklee *et al.*[16] In the VSL technique, luminescence from the sample, excited within the pumped stripe-shaped area of the length l, serves as the probing beam. Light passing through the excited area of a reasonable length l enables the stimulated emission. However, interpretation of the VSL data in low-gain materials is less straightforward and several gainlike artifacts can mask the real gain effects.[17,18,21,22] Lourenço *et al.*[23] proposed a technique for low-gain measurements in short waveguides in a geometry similar to VSL. In this configuration, the sensitivity to low gains was improved, but the aforementioned artifacts, arising mainly from the discrepancy between the one-dimensional VSL model and the real system geometry and/or waveguiding effects, could not be fully eliminated.

The sensitivity to low optical gains can be also improved by use of the VSL in combination with the SES technique.[17] Due to its comparative character, this method enables to resolve even a small optical gain under conditions when no net gain can be observed and corrects the signal for most of the possible artifacts. It is also suitable for nonwaveguiding samples. Nevertheless we feel important to note that VSL-like techniques use "stripe-shaped" pumped area and therefore, for a precise interpretation of the observed results in low-gain materials, laser-induced changes in the refractive index should be taken into account.

In this paper, laser-induced changes in the absorption coefficient are studied using the combination of the VSL and SES. The measurements were conducted at low temperature ($T=4.2$ K) under cw and pulsed laser excitation, both at 532 nm. The cw excitation was provided by a solid-state laser $Nd:YVO_4$ (Spectra Physics) and the pulsed excitation by a third harmonic of a Nd:YAG laser pumping a tunable wavelength optical parametric oscillator (Solar Laser Systems), featuring 5-ns pulses with a repetition rate of 20 Hz. The detection system and cryostat configuration remain the same as for PL measurements.

In the VSL experiment, sample is excited by a homogeneous stripelike intense laser beam [Fig. 1(a)] of a length l, formed by a cylindrical lens. In order to achieve a homogeneous excitation, only a part of the Gaussian profile of the excitation beam is used, selected by the slit of 1.2-mm width, placed before the cylindrical lens. The length of the VSL stripe is changed by a moving shield (with a sharp-edge knife) placed on a motorized micropositioner with the resolution of 1.25 μm. For the SES experiment, another blocking shield is introduced to the VSL setup [Fig. 1(b)] in order to create a small rectangular excited spot that can be shifted along the stripe as used in the VSL configuration. The width of the SES spot x_0 is equal to the differential shift of the slit in the VSL setup (Fig. 1). In order to minimize the effect of the inevitable laser diffraction on the movable shields on the spot/stripe shape, a double-lens system with the magnification ratio of 2.5:1 was placed in front of the sample. The Er-1 related 1.54 μm PL is detected from the edge of the sample, perpendicularly to the excitation (Fig. 1).

In the SES experiment, PL emerging from the excited spot passes through a nonexcited area of length $l_k = kx_0$ [$k=0,\ldots,n$; Fig. 1(b)], where it can be absorbed by Er-1 centers in the ground state. The signal attenuation is given by the absorption coefficient of Er-1 centers in the ground state α_0. Scattering losses as well as absorption of the ultranarrow Er-1 center emission line at 1.54 μm by other Er dopants, if any, can be neglected due to their broad absorption spectra.

The detected SES signal follows the Beer-Lambert law

$$I_k^{\mathrm{SES}} = I_{SpE} e^{-\alpha_0 l_k}, \tag{1}$$

where I_{SpE} stands for the spontaneous emission intensity per unit length.

Let us now discuss the situation, when the luminescence passes the system where all the Er-1 centers are in the excited state, which can be realized by measuring the VSL in the saturation regime. Under such conditions, laser-induced absorption coefficient α_{ind} comprises the optical gain g (negative absorption coefficient of Er-1 in the excited state) and the free carrier absorption α_{FCA}. The detected VSL signal is given by

$$I_k^{\mathrm{VSL}} = I_{SpE} \frac{1 - e^{-\alpha_{ind} l_k}}{\alpha_{ind}},$$

$$\alpha_{ind} = \alpha_{FCA} - g. \tag{2}$$

The negative value of α_{ind} would lead to light amplification, defined by the net gain coefficient $G = |\alpha_{ind}|$. The positive value, on the other hand, would lead to attenuation and could appear in the situation when the free carrier absorption dominates over the stimulated emission ($\alpha_{FCA} > g$). Since the free carrier absorption cross section in c-Si at 1.54 μm is known [$\sigma_{\mathrm{Si}} \sim 10^{-17}$ cm^2 (Refs. 24 and 25)], one can estimate g from comparison of measured α_{ind} and α_{FCA}.

Laser-induced changes in absorption coefficient $\Delta\alpha = \alpha_{ind} - \alpha_0$ result in a difference between the as-measured VSL signal I_k^{VSL} and the SES signal $I_k^{i\mathrm{SES}}$, integrated over the stripe length l_k

$$I_k^{i\mathrm{SES}} = \sum_{j=1}^{k} I_j^{\mathrm{SES}}. \tag{3}$$

In saturation (all Er-1 centers in the excited state), the α_0 magnitude determines the maximal optical gain coefficient $g = |\alpha_0|$ of the Er-1 center, leading to $\Delta\alpha = \alpha_{FCA} - 2g$. The magnitude of $\Delta\alpha$ can be evaluated from comparison of the as-measured SES signal I_k^{SES} with the differential VSL signal $I_k^{d\mathrm{VSL}}$

$$I_k^{d\mathrm{VSL}} = \frac{I_k^{\mathrm{VSL}} - I_{k-1}^{\mathrm{VSL}}}{x_0} = I_{SpE} e^{(g - \alpha_{FCA}) l_k} \tag{4}$$

leading to

$$\Delta\alpha = -\frac{\ln(I_k^{d\mathrm{VSL}} / I_k^{\mathrm{SES}})}{l_k} = \alpha_{ind} - \alpha_0. \tag{5}$$

In both cases, size of the SES spot must be carefully adjusted to be equal to the VSL differential shift step x_0 (Fig. 1).

III. EXPERIMENTAL RESULTS

The PL spectrum of the Si/Si:Er multinanolayer structure, measured at $T = 4.2$ K under cw 532 nm excitation, is plotted in Fig. 2(a). The spectrum features few intense lines (indicated by the arrows) and arises from the radiative recombination from the lowest level of the first excited state into the split ground state of Er^{3+} in the slightly distorted tetrahedral position [inset in Fig. 2(a)].[11] In this study we concentrate on the nonlinear optical properties of the ultranarrow Er-1 center emission peak at $\sim$1.54 μm [Fig. 2(b)].

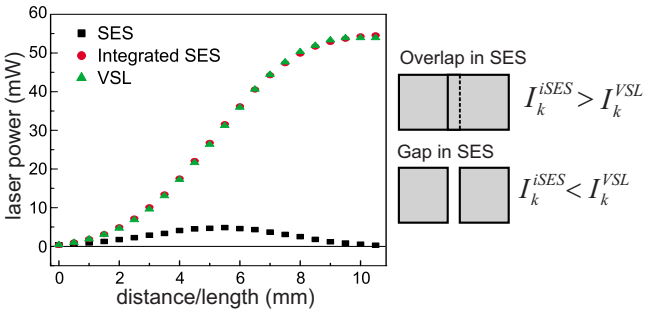

FIG. 3. (Color online) (Left) Gaussian excitation beam profile of the cw laser at 532 nm, measured immediately after the movable shields in the SES and VSL setups. (Right) Sketch of the nonideal situation when $x_0^{\mathrm{SES}} > x_0^{\mathrm{VSL}}$ (spot overlap) or $x_0^{\mathrm{SES}} < x_0^{\mathrm{VSL}}$ (gap between spots), leading to a difference in the integrated SES and VSL signals, i.e., artificial $\Delta\alpha \neq 0$.

Prior to the nonlinear absorption coefficient investigations, the excitation beam profile and equality of the SES spot size with the VSL differential shift has been verified (to avoid an overlap or a gap between the SES spots). For this purpose, a power meter has been placed immediately after the movable shields and signals at the excitation wavelength of 532 nm have been measured in the SES and VSL configurations (Fig. 3). The integrated SES $I_k^{i\mathrm{SES}}$ and the as-measured VSL signal I_k^{VSL} of the laser beam in Fig. 3 are identical, which confirms equality of the SES spot size (x_0^{SES}) and the differential VSL shift step ($x_0^{\mathrm{VSL}} = x_0^{\mathrm{SES}} \equiv x_0$; Fig. 1) and validates the experimental procedure. The as-measured SES signal in Fig. 3 copies the excitation beam profile. However, as mentioned before, in the optical gain experiment only a short central part of the beam, of a width of $\sim$2 mm and a flat profile, has been used (additional slit) in order to achieve a homogeneous excitation beam profile.

Also a possible effect of the focal point of the PL collecting lenses has been considered. To ensure the constant efficiency of the detection over the whole stripe length ($<$1.5 mm), a large monochromator detection slit of 2 mm was used. Moreover, the change in the detected signal intensity with a slight ($\pm$1 mm) shift of the objective lens has been checked and found to be negligible. That is understandable, since the objective lens numerical aperture is small (NA $\approx$ 0.24). Moreover, this effect is automatically corrected in the SES and VSL comparison.

As discussed above, the signals of the integrated SES and VSL should match each other in the case that $\Delta\alpha = 0$. We note, however, that in spite of this careful calibration, a difference between VSL and SES experiments with Er-1 emission may still appear not necessarily due to the nonlinear effects. In particular, some electrons and holes generated within the illuminated spot can diffuse out of the excitation region, contributing additional Er-1 luminescence. Such a situation is especially plausible at higher excitation fluxes. Consequently, the integrated SES signal might be overestimated. This experimental artifact can mask a small optical

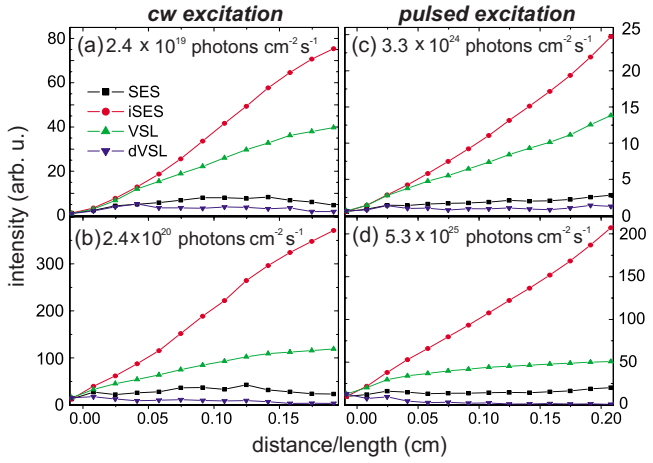

FIG. 4. (Color online) Comparison of the as-measured VSL and SES signals with the integrated SES and differential VSL signals, measured at 1.54 μm Er-1-related emission for different excitation flux under [(a) and (b)] cw and [(c) and (d)] pulsed excitation at 532 nm. Measurements were done at low temperature $T=4.2$ K.

gain, which might actually appear in the case that equal SES and VSL signals are being measured. However, it is important to note that this effect can lead to a possible underestimation of the gain coefficient and never to an overestimation.

In Figs. 4(a)–4(d) we show a comparison of the as-measured VSL and SES signals with the integrated SES and differential VSL signals at 1.54 μm, measured for the sample under [(a) and (b)] cw and [(c) and (d)] pulsed excitation at 532 nm, $T=4.2$ K, and two selected photon fluxes.

IV. DISCUSSION

Laser-induced changes in absorption coefficient $\Delta\alpha$ were evaluated using Eq. (5) from comparison of the as-measured SES and the differential VSL signal. The result is plotted in Figs. 5(a) and 5(b).

Since the laser-induced absorption coefficient α_{ind} strongly depends on the excitation conditions, measurements were done for various excitation fluxes in pulsed and cw regimes. In particular, in order to reach the upper gain limit

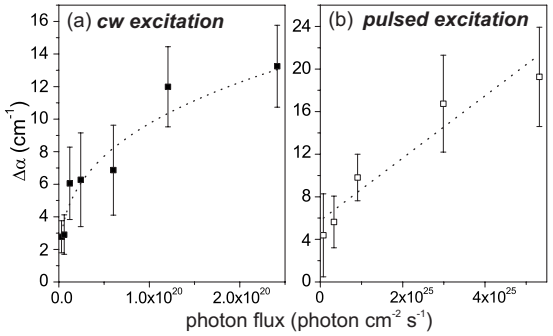

FIG. 5. Laser-induced absorption coefficient changes $\Delta\alpha$ as function of the excitation photon flux Φ for both (a) cw and (b) pulsed excitation ($t_p=5$ ns) at 532 nm. The dashed lines represent fits by Eqs. (7) and (9), respectively.

condition, the saturation of PL must be achieved. Therefore, high pump fluxes Φ, on the order of $3\times10^{18}-2\times10^{20}$ photons cm^{-2} s^{-1}, were applied for the cw excitation [Fig. 5(a)] and $7\times10^{23}-5\times10^{25}$ photons cm^{-2} s^{-1} for the pulsed excitation [Fig. 5(b)], both at 532 nm. Experiments were done also under different excitation wavelengths (469, 489, 630 nm) in pulsed regime. Since the observed results are very similar, we do not present these data here.

As mentioned before, stimulated emission at 1.54 μm in our system competes with high free carrier absorption α_{FCA}. Under high cw excitation flux, the free carrier absorption is maximal, as is the effect of the optical gain. In Figs. 4(a) and 4(b) we show the VSL and SES data measured under such a condition. It can be clearly seen that the integrated SES signal is higher than the corresponding VSL signal. This difference increases with higher flux and longer stripe length. Similar behavior has been observed also for different pump fluxes (data not presented). This implies that laser-induced losses dominate, i.e., $\Delta\alpha>0$ (Fig. 5).

In order to evaluate the laser-induced absorption cross-section, kinetic model for concentration of free carriers (including free excitons) n in a system of silicon and erbium is used

$$\frac{dn(t)}{dt} = \alpha\Phi - \frac{n}{\tau_{FC}},$$

$$\tau_{FC}^{-1} = \tau_{trap}^{-1} + \tau_{rad}^{-1} + \tau_{Auger}^{-1}. \tag{6}$$

Here α stands for the absorption coefficient of the system at the excitation wavelength; τ_{trap}^{-1} is the trapping rate; $\tau_{rad}=n\beta$ is the radiative recombination rate given by the radiative coefficient β [in crystalline silicon $\sim1.1\times10^{-14}$ cm^3 s^{-1} (Ref. 26)]; $\tau_{Auger}^{-1}=n^2\gamma$ stands for the Auger recombination rate given by Auger coefficient γ [in crystalline silicon $\sim2.8\times10^{-31}$ cm^6 s^{-1} (Ref. 27)]. The thermal generation of free carriers is neglected since the VSL and SES measurements were performed at $T=4.2$ K.

Under cw excitation, Eq. (6) can be solved for the steady-state condition. Moreover, high flux regime leads to saturation of trapping to Er and other possible defect states. Also radiative transitions in this structure can be neglected compared to the nonradiative Auger recombination, simplifying the Eq. (6) to $(dn/dt)=0\approx(\alpha\Phi-n^3\gamma)$ and leading to a cubic-root dependence of the free carrier density on the pump flux:

$$n_{\mathrm{cw}} = \sqrt[3]{\frac{\alpha}{\beta}\Phi}. \tag{7}$$

The coefficient of the laser-induced changes in absorption $\Delta\alpha$ is given as

$$\Delta\alpha = \sigma n. \tag{8}$$

Using the Eqs. (7) and (8) and the known value of absorption of c-Si at the excitation wavelength $\alpha(532\ \mathrm{nm})=6800$ cm^{-1},[28] we obtain laser-induced absorption cross section $\sigma_{\mathrm{cw}}=(1.12\pm0.06)\times10^{-17}$ cm^2 [fit in Fig. 5(a)]. This value is in excellent agreement with the usually observed free carrier cross section in c-Si $\sigma_{\mathrm{Si}}\sim10^{-17}$ cm^2,[24,25] implying that the gain (if any) is much smaller. Therefore we can

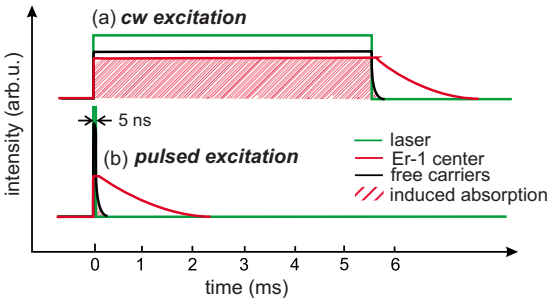

FIG. 6. (Color online) Sketch of the interplay between the free carriers and Er-1 luminescence lifetimes under laser illumination for (a) cw and (b) pulsed excitation (t_p=5 ns). The striped areas represent the induced absorption at the emission wavelength of 1.54 μm due to the free carrier absorption.

conclude that in order to enhance the effect of stimulated emission, free carrier effects must be drastically lowered.

In order to lower α_{FCA}, a short pulsed laser excitation would be advantageous. The pulse duration t_p should be smaller than Er-1 related luminescence decay time and free carriers lifetime τ_{FC}. In the pure c-Si at cryogenic temperatures, τ_{FC} can be as high as 1 ms, which is comparable to the luminescence lifetime of Er-1 center.[20] However, in highly doped silicon, trapping radically reduces τ_{FC} to the nanosecond range.[29,30] The exciton lifetime (at $\sim$1.14 μm) in our Si/Si:Er multinanolayer structure was measured to be 150 ns by photon counting method (data not shown) at low temperature ($\sim$15 K, closed-cycle cryostat).

The VSL and SES data, measured with the pulsed excitation (t_p=5 ns), are plotted in Figs. 4(c) and 4(d). The evaluated $\Delta\alpha$ given in Fig. 5 is lower than that measured with cw excitation (note the different excitation photon flux).

The solution of Eq. (6) for short ($t_p \ll \tau_{FC}$) intense pulses leads to a simple linear dependence

$$n_{pulse} \approx \alpha \Phi t_p. \tag{9}$$

The linear fit of the laser-induced losses $\Delta\alpha$ on the excitation photon flux in Fig. 5(b), using Eq. (9), leads to $\sigma_{pulse}=(8.6\pm1.7)\times10^{-21}$ cm^2.

Assuming that only the free carrier losses are present, losses induced under excitation flux used in pulsed experiment should be several orders of magnitude higher than experimentally measured [Fig. 5(b)]. However, σ_{pulsed} is significantly lowered, compared to σ_{cw}. This can be related to the short free carrier lifetime, compared to the Er-1 related luminescence, which makes the free-carriers effects to become negligible under the pulsed excitation, compared to the cw excitation.

The sketch of the interplay between the free carriers and Er-1 luminescence lifetimes is shown in Fig. 6. Under pulsed excitation, the effect of the optical gain is greatly enhanced, lowering the measured induced absorption cross section from expected $\sigma_{\mathrm{Si}}\sim10^{-17}$ cm^2 down to $\sigma_{pulse}=(8.6\pm1.7)\times10^{-21}$ cm^2. Optical gain cross section in our system from Er-1 related emission can then be estimated as $\sigma_{gain}=\sigma_{\mathrm{Si}}-\sigma_{pulse}\leq10^{-17}$ cm^2. Under the given experimental conditions, when all optically active Er-1 centers are in the excited state, σ_{gain} represents the upper limit of the optical gain. Considering the concentration of the optically active Er dopants (Er-1 centers) of $\sim8.8\times10^{17}$, we achieve the upper limit of the optical gain coefficient g=8.8 cm^{-1}. If all free carrier absorption losses could be eliminated, this would correspond to a net gain coefficient G of 38.2 dB cm^{-1}. Compared to the value estimated in Ref. 23 (g=22 dB cm^{-1} expected for Er concentration of 10^{19} cm^{-3}), we achieved nearly 20 times higher value. This is reasonable, since Ref. 23 (i) gives the lower limit and (ii) the investigated Er emission was inhomogeneously broadened. On the other hand, our estimate is lower than could be expected from linewidth comparison ($\sim10^3$).

While the upper limit of the optical gain cross section is reasonably high, free carrier losses exceed the stimulated emission effect even at the optimum conditions, such as ultranarrow emission line, cryogenic temperature, saturation regime, and short pulse excitation. Therefore we conclude that net optical gain in Er-doped silicon will only be possible if the free carrier losses will be severely suppressed. One possibility to achieve that could be by an application of electric field to drive away free carriers immediately after excitation of Er^{3+} ions, i.e., following a strategy similar to that used in Ref. 1.

V. CONCLUSION

The present study demonstrates that comparison of differential VSL and as-measured SES signal can be used for determination of laser-induced absorption cross section. This technique was applied to study optical gain and free carrier absorption at Er-1 related ultranarrow emission line at 1.54 μm in MBE grown Si:Er material. Under high flux cw excitation, when the free carrier effects are maximal, the measured laser-induced absorption cross section at 1.54 μm agreed well with that commonly reported for free carriers in c-Si. Under pulsed excitation, on the other hand, free carrier effects are minimized while stimulated emission remains intact. Under such conditions, considerable lowering of the laser-induced absorption cross section has been observed. From that the upper limit of optical gain in Er-doped silicon was estimated as 8.8 cm^{-1}. We conclude that free carrier influence must be drastically lowered if net gain is to be achieved in c-Si:Er.

ACKNOWLEDGMENTS

This work was supported by The Foundation for Fundamental Research on Matter (FOM) and the Netherlands Organisation for Scientific Research (NWO). We thank Z. F. Krasil'nik from Russian Academy of Sciences (Nizhny Novgorod, Russia) for loan of the sample.

*n.h.ngo@uva.nl
†On leave from Institute of Physics, Academy of Sciences of the Czech Republic, v.v.i., Cukrovarnická 10, CZ-162 53 Prague 6, Czech Republic.

[1] H. Rong, R. Jones, A. Liu, O. Cohen, D. Hak, A. Fang, and M. Paniccia, Nature (London) **433**, 725 (2005).
[2] J. H. Park and A. J. Steckl, J. Appl. Phys. **98**, 056108 (2005).
[3] A. Polman, B. Min, J. Kalkman, T. J. Kippenberg, and K. J. Vahala, Appl. Phys. Lett. **84**, 1037 (2004).
[4] T. J. Kenyon, Semicond. Sci. Technol. **20**, R65 (2005).
[5] A. Polman, G. N. Vandenhoven, J. S. Custer, J. H. Shin, R. Serna, and P. F. Alkemade, J. Appl. Phys. **77**, 1256 (1995).
[6] T. Gregorkiewicz, D. T. X. Thao, and J. M. Langer, Appl. Phys. Lett. **75**, 4121 (1999).
[7] M. Forcales, T. Gregorkiewicz, I. V. Bradley, and J.-P. R. Wells, Phys. Rev. B **65**, 195208 (2002).
[8] O. B. Gusev, M. S. Bresler, P. E. Pak, I. N. Yassievich, M. Forcales, N. Q. Vinh, and T. Gregorkiewicz, Phys. Rev. B **64**, 075302 (2001).
[9] T. Gregorkiewicz and J. M. Langer, MRS Bull. **24**, 27 (1999).
[10] N. Q. Vinh, N. N. Ha, and T. Gregorkiewicz, IEEE Int. Reliab. Phys. Symp. Proc. **97**, 1269 (2009).
[11] N. Q. Vinh, H. Przybylińska, Z. F. Krasil'nik, and T. Gregorkiewicz, Phys. Rev. Lett. **90**, 066401 (2003).
[12] N. Q. Vinh, H. Przybylińska, Z. F. Krasil'nik, and T. Gregorkiewicz, Phys. Rev. B **70**, 115332 (2004).
[13] G. N. van den Hoven and J. H. Shin, J. Appl. Phys. **78**, 2642 (1995).
[14] S. Takeoka, M. Fujii, and S. Hayashi, Phys. Rev. B **62**, 16820 (2000).
[15] A. Koizumi, Y. Fujiwara, A. Urakami, K. Inoue, T. Yoshikane, and Y. Takeda, Appl. Phys. Lett. **83**, 4521 (2003).
[16] K. L. Shaklee and R. F. Leheny, Appl. Phys. Lett. **18**, 475 (1971).
[17] J. Valenta, I. Pelant, and J. Linnros, Appl. Phys. Lett. **81**, 1396 (2002).
[18] J. Valenta, K. Luterová, R. Tomasiunas, K. Dohnalová, B. Hönerlage, and I. Pelant, *Towards the first silicon laser*, NATO Science Series II: Mathematics, Physics and Chemistry Vol. 96, edited by L. Pavesi, S. Gaponenko, and L. Dal Negro (Kluwer, Dordrecht, 2003), p. 223.
[19] B. A. Andreev, A. Yu. Andreev, H. Ellmer, H. Hutter, Z. F. Krasil'nik, V. P. Kuznetsov, S. Lanzerstorfer, L. Palmetshofer, K. Piplits, R. A. Rubtsova, N. S. Sokolov, V. B. Shmagin, M. V. Stepikhova, and E. A. Uskova, J. Cryst. Growth **201-202**, 534 (1999).
[20] N. Q. Vinh, S. Minissale, H. Vrielinck, and T. Gregorkiewicz, Phys. Rev. B **76**, 085339 (2007).
[21] L. Dal Negro, M. Cazzanelli, N. Daldosso, Z. Gaburro, L. Pavesi, F. Priolo, D. Pacifici, G. Franzò, and F. Iacona, Physica E **16**, 297 (2003).
[22] T. Ostatnický, P. Janda, J. Valenta, and I. Pelant, Proc. SPIE **6609**, 66090F (2007).
[23] M. A. Lourenço, R. M. Gwilliam, and K. P. Homewood, Appl. Phys. Lett. **91**, 141122 (2007).
[24] W. B. Gauster and J. C. Bushnell, J. Appl. Phys. **41**, 3850 (1970).
[25] W. Spitzer and H. Y. Fan, Phys. Rev. **108**, 268 (1957).
[26] W. Gerlach, H. Schlangenotto, and H. Maeder, Phys. Status Solidi A **13**, 277 (1972).
[27] J. Dziewior and W. Schmid, Appl. Phys. Lett. **31**, 346 (1977).
[28] *Properties of Crystalline Silicon*, Data Reviews Series No. 20, edited by R. Hull (INSPEC, London, UK, 1999), p. 677.
[29] D. L. Adler, D. C. Jacobson, D. J. Eaglesham, M. A. Marcus, J. L. Benton, J. M. Poate, and P. H. Citrin, Appl. Phys. Lett. **61**, 2181 (1992).
[30] K. R. Lea, M. J. M. Leask, and W. P. Wolf, J. Phys. Chem. Solids **23**, 1381 (1962).